Nucleation and growth of eutectic cell in hypoeutectic Al−Si alloy

SUN Yu[1], PANG Shao-ping[1], LIU Xue-ran[1], YANG Zi-run[1], SUN Guo-xiong[2]

1. School of Materials Engineering, Yancheng Institute of Technology, Yancheng 224002, China;
2. School of Materials Engineering, Southeast University, Nanjing 210096, China

Abstract: The nucleation and growth of eutectic cell in hypoeutectic Al−Si alloy was investigated using optical microscopy and scanning electron microscopy equipped with electron backscattering diffraction (EBSD). By revealing the eutectic cells and analyzing the crystallographic orientation, it was found that both the eutectic Si and Al phases in an eutectic cell were not single crystal, representing an eutectic cell consisting of small 'grains'. It is also suggested that the eutectic nucleation mode can not be determined based on the crystallographic orientation between eutectic Al phases and the neighboring primary dendrite Al phases. However, the evolution of primary dendrite Al phases affects remarkably the following nucleation and growth of eutectic cell. The coarse flake-fine fibrous transition of eutectic Si morphology involved in impurity elements modification may be independent of eutectic nucleation.

Key words: hypoeutectic Al−Si alloy; eutectic cell; nucleation; growth

1 Introduction

The hypoeutectic Al−Si alloys, due to their excellent castability, corrosion resistance and higher specific strength in the heat-treated condition, are most widely used in automotive and aerospace industries [1−3]. Microstructure evolution of hypoeutectic Al−Si alloys during solidification is in two stages: primary dendrite Al phase formation, and the subsequent eutectic transformation. Based on the Al−Si binary diagram, the volume fraction of Al−Si eutectic in commonly used hypoeutectic Al−Si alloys, such as A356, A357, can be more than 50%. With small addition of impurity elements, the eutectic Si undergoes a morphological transition from coarse flake to fine fibers, improving the mechanical properties of Al−Si alloy. In the past years, the modification mechanism has always been paid close to the materials researchers [4−9].

Recently, it is popular to investigate the formation of eutectic cell (eutectic grain), involving nucleation and growth. Using EBSD, NOGITA et al [10−11] suggested that in unmodified hypoeutectic Al−Si alloys, the eutectic nucleated on primary dendrites because of the same orientation between the eutectic Al phase and the surrounding primary dendrite Al phases. However, when the modified alloys with small quantity of Sr (e.g., 0.011%), the eutectic nucleated within the interdendritic liquid, i.e., the eutectic Al phase did not have the same orientation as surrounding primary dendrite Al phases. It is interesting to note that at higher Sr content (e.g., 0.5%) the eutectic reverted back to nucleating on the primary dendrite Al phases. More compelling evidence demonstrated through TEM that the eutectic in hypoeutectic Al−Si alloy nucleated on the secondary β-(Al, Si, Fe) phase in the solute field ahead of the growing dendrite Al phases [12], and no crystallographic relationship was found between the primary dendrite Al phases and the eutectic. McDONALD et al [13−14] found that the addition of Sr to the commercial Al−10%Si alloy reduced the number of eutectic grains. The size of eutectic grains in unmodified commercial alloy, at a cooling rate of about 1.65 K/s, was too small to be resolved, and a macrograph of the 0.019% Sr-modified alloy quenched partway through eutectic solidification had very large eutectic grains of more than 2 000 μm because of decreasing the eutectic nucleation density. Meanwhile, he pointed out further that it was impossible for eutectic to nucleate on primary dendrite Al phases. LIAO et al [15−16] found that the eutectic

grain size decreased with increasing Sr content because the addition of Sr led to a depression of eutectic temperature in Al−Si alloy, and hence, the nucleating driving of eutectic cell was increased. So the number of nuclei of eutectic was increased.

There are some conflicting views and lack of understanding as to how the eutectic forms. The present work was conducted to gain further understanding about the nucleation and growth of eutectic cells in hypoeutectic Al−Si alloy. The microstructures were characterized by optical microscope and scanning electron microscope (SEM) equipped with electron backscattering diffraction (EBSD).

2 Experimental

Al−10%Si alloy, the composition of which is shown in Table 1, was melted in an electrical resistance furnace using a graphic crucible, from ZAlSiD-0 and 99.5% commercial pure Al. Al−4.85%Sr master alloy was added into the melt at 730 °C. After holding for 30 min, TR-L-CJ flux was introduced for degassing. Then, the melt was poured at 720 °C into firebrick mould and metallic mould (45$^{\#}$ steel, which was preheated to 200 °C) respectively. Cylindrical casting with 20 mm in diameter and 60 mm in height was obtained.

Table 1 Compositions of Al−10%Si alloys (mass fraction, %)

Si	Fe	Mg	Cu
10.20	0.16	0.015	0.003
Mn	Zn	Ti	Al
0.003	≤0.019	≤0.007	Balance

Metallographic samples were cut from the middle of the casting samples. An improved aqueous solution of $K_3Fe(CN)_6$ was prepared for revealing the eutectic cells. The microstructure was characterized by optical microscope (OLYMPUS, BX−60M).

The ESBD specimen was prepared by the following method. Sample with thickness of less than 0.5 mm was obtained with linear cutting, then was punched to 3 mm in diameter and polished up to 0.5 μm polishing. Ion milling was carried out with Ar^+ ions under the following conditions: 1.5−2 h at a voltage of 4 V and gun tilt angle of 15°, and cooling by liquid nitrogen during the milling.

EBSD examination was conducted in a Sirion scanning electron microscope (SEM) equipped with an electron backscattering diffraction (EBSD, OIM400) instrument, which characterized the crystallographic orientation of different phases. The TSL software of EBSD system allowed for fully automated recording and indexing of diffraction patterns, and the orientation data were stored in a computer. In order to obtain clear EBSD mapping, the scanning step length was set at 0.3 μm, and about 350 000 effective data points were collected in the present work.

3 Results and discussion

3.1 Morphology of Al-Si eutectic cell

Figure 1 shows the microstructures of Al−10%Si alloy modified by 0.025% Sr, which contains the primary dendrite Al phase (white) and eutectic (black). In the eutectic region, the morphology of eutectic cells was observed clearly. The long columnar eutectic cells were observed in metal mould sample, as shown in Fig. 1(a), whose length and width are 200−350 μm and 60−100 μm, respectively. Correspondingly, the near-equiaxed eutectic cells were observed in firebrick mould sample, as shown in Fig. 1(b), whose equivalent size was 300−500 μm. HUNT [17] proposed a general model of CET (columnar-equiaxed transformation), which is also applicable to eutectic growth. At the higher thermal gradient (metal mould) in the front of solid-liquid interface during solidification, the eutectic cells developed in columnar manner. Conversely, the eutectic cells had a tendency to grow in the equiaxed manner (firebrick mould). The result indicated that the eutectic cell character depends mainly on solidification conditions.
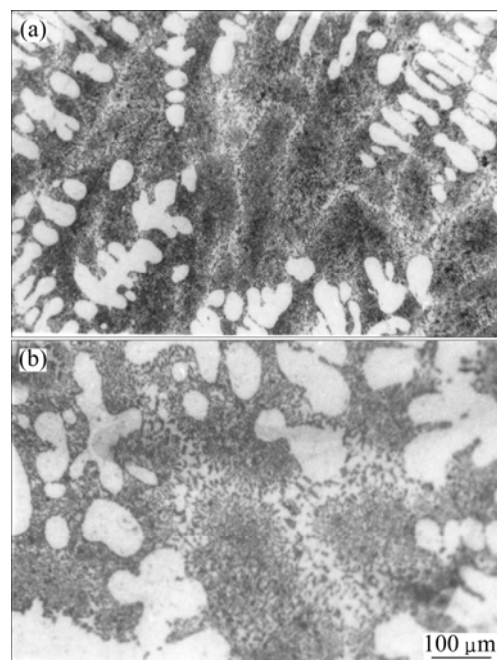

Fig. 1 Microstructures of Al−10%Si alloys modified by 0.025% Sr: (a) Metal mould sample; (b) Firebrick mould sample

3.2 EBSD analysis

Figure 2 shows the secondary electron image of Al−10%Si alloy modified by 0.025% Sr and
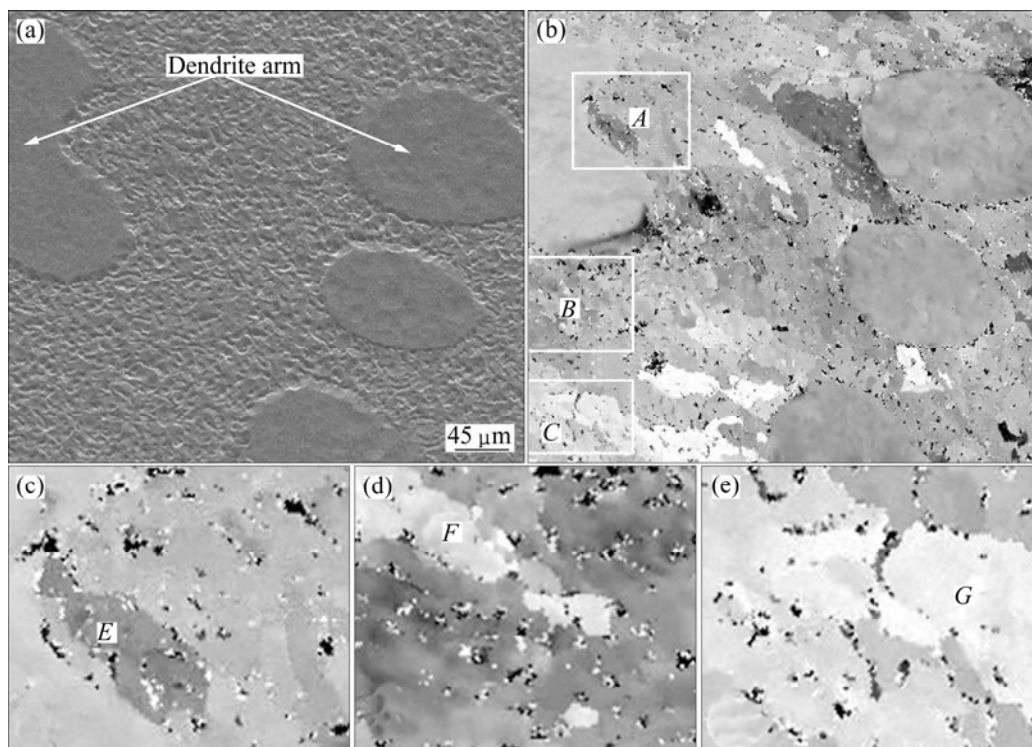
Fig. 2 Secondary electron image (a) of Al−10%Si modified by 0.025% Sr and corresponding EBSD orientation mapping (firebrick mould) (b) and EBSD patterns of zones *A* (c), *B* (d) and *C* (e) in Fig. 2(b)

corresponding EBSD orientation mapping. A well-modified eutectic structure was readily observed. On the EBSD mapping, the different grey scales indicate different crystallographic orientations. Black regions (or points) are the results of insufficient orientation information, usually correlating with Si particles which often cause a 'shaded/deformed' diffraction pattern of which the system cannot be indexed. It should be noted that the EBSD patterns from aluminum and silicon are very similar since aluminum is a face-centered cubic structure and silicon is a diamond cubic structure, as shown in Fig. 3. The EBSD program was set for indexing of diffraction pattern from Al phase, although the orientations from silicon can also be obtained simultaneously.

The eutectic region was surrounded by several primary Al dendrite arms. Some small 'grains' were observed in the eutectic region and appeared as irregular elongated or columnar character, as shown in the partial enlarged drawing labeled *A*, *B* and *C* in Fig. 2(b). The grey scales of labeled *E*, *F* and *G* areas were not identical with that of surrounding, a wide range of different orientations were observed within the eutectic region, representing a structure consisting of small 'grains'. By comparison with Fig. 1(b), the small 'grains' shown in EBSD mapping may not be an independent eutectic cell.
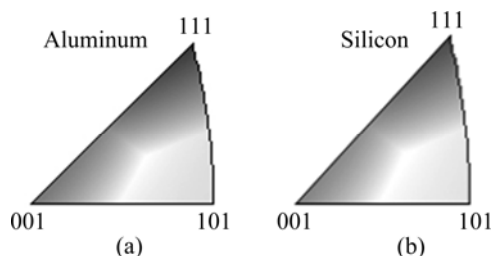

Fig. 3 Grey scale coded map type of Al (a) and Si (b) phases in inverse pole figure

The concept of eutectic cell originates from the gray cast-iron. For the Al−Si alloy, the eutectic cell in Al−Si alloy should be considered the eutectic Si as well as branches from one eutectic nucleus together with the coupled-growth eutectic Al phases. It is widely accepted that the eutectic Si phase is the 'leading phase' in the growth, which is a successive framework in an eutectic cell. Therefore, the morphology of eutectic cell depends upon the growth of eutectic Si phase in each aspect [18]. The three-dimensional morphology of eutectic Si in Al−10%Si alloy modified by 0.025% Sr is shown in Fig. 4 (the sample was deeply etched to remove Al matrix). It was found that the irregular eutectic Si and branches had no rational or consistent growth axes. The 'leading Si phase' changed constantly itself growth direction (or forming new branches) by inducing the growth of twins

with the addition of modification elements [4]. As a result, the metal matrix (eutectic Al phase) was forced to adjust itself growth direction or repeatedly nucleate on Si phase to adapt a new epitaxial orientation as fast as growth proceeds. So it is beneficial to decreasing the interface energy of eutectic Al and Si phases or keeping a more closely coupled growth. It was due to the variation of growth orientations of the 'leading Si phase' together with the coupled-growth eutectic Al phases, resulting in the irregular elongated or columnar 'grains' observed in the EBSD mapping. It is further to demonstrate that an eutectic cell is composed of some small 'grains' with different crystallographic orientations, as illustrated in Fig. 5. The results also suggest that both the eutectic Si and Al phases in an eutectic cell are not single crystal.
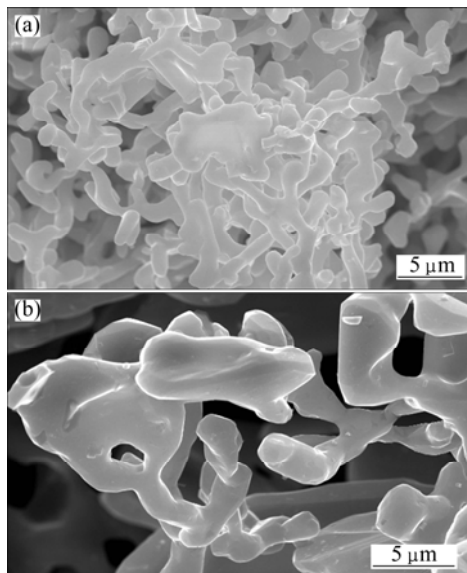

Fig. 4 Morphologies of Si dendrite in Al−10%Si alloy modified by 0.025% Sr (3-D): (a) Lower magnification; (b) Higher magnification
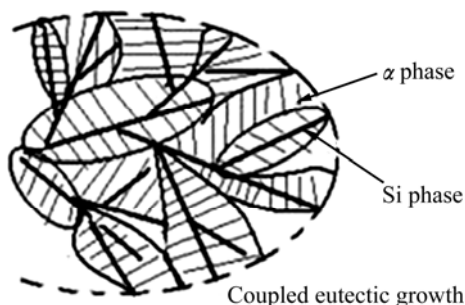

Fig. 5 Schematic illustration of eutectic cell model

The orientation differences of the eutectic Al phases and the neighboring primary dendrite Al phases were also measured using the TSL software in the present work, which changed usually in the range of 2.3°−18.1°

(individual was excess of 38.3°). The result was in good agreement with the observation from NOGITA et al [10−11]. However, they thought that, in this case, the eutectic nucleated within the interdendritic liquid. As observed and discussed above, the eutectic nucleation mode was not determined because of the varying crystallographic orientation of the eutectic Al phase in an eutectic cell. In fact, even if the location orientation is identical, it is also difficult to determine the eutectic nucleation mode. For the (Al +Si) eutectic, Si is the "leading phase" and needs to nucleate before eutectic growth occurring. It was reported that eutectic Si can nucleate on existing heterogeneous substrates in the melt, such as AlP and other potent unknown nuclei, which become activated at a certain degree of undercooling. The nuclei for eutectic Si can be pushed on ahead of the growing dendrite-liquid interface during solidification. Once nucleating, the eutectic Si grows into eutectic liquid. The liquid surrounding the eutectic silicon Si becomes enriched in Al atoms as it is being depleted of Si. Consequently, eutectic Al phase nucleates and grows on the edges and tips of the eutectic Si. Finally, the aluminum dendrites stop growing upon impingement with the growing eutectic aluminum cells. In this case, it is possible that the part of eutectic Al phases have the same crystallographic orientation as surrounding primary dendrite Al phases.

3.3 Effect of dendrite refinement on eutectic cell

For the hypoeutectic Al−Si alloy, it is necessary to refine the primary dendrite Al phase, as well as to modify eutectic Si, in order to obtain ever-improving mechanical properties. The Zr compound salt was added into the melt of Al−10%Si alloy in the present experiment. The detailed process may refer to Ref. [19].

Figure 6 shows the microstructures of 0.025% Sr modified Al−10%Si alloy with the addition of Zr compound salt (about 0.25% Zr in the alloy). In comparison with Fig. 1, the addition of Zr compound salt led to a transition of primary dendrite Al phase from columnar to fine equiaxed. Zr is an effective grain refinement element (only inferior to Ti) for Al alloys. ZrAl$_3$ particles from the reaction of Al melt and Zr compound salt were an effective heterogeneous substrate for primary dendrite Al phase [19]. It was also observed that the fine, well-distributed and equiaxed eutectic cells were also observed with the refinement of primary dendrite Al phases. The size of eutectic cell was in the range of 20−50 μm in metal mould sample and 60−100 μm in firebrick mould sample. The result indicates that a large population of potential nuclei in melt may be activated. It is not confirmed the other reactants, being from Al melt and Zr compound salt, whether or not as effective nuclei for the "leading Si phase" in eutectic.

However, it is evident from the results that the evolution of primary dendrite Al phase may affect the subsequent nucleation and growth of eutectic.
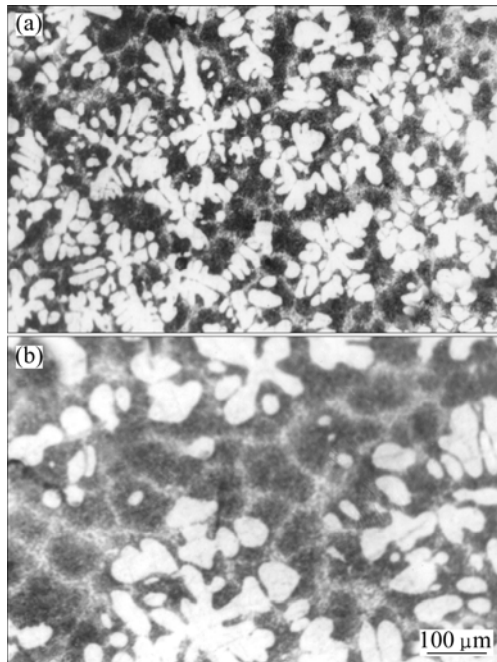

Fig. 6 Microstructures of 0.025% Sr modified Al−10%Si alloy with addition of Zr compound salt: (a) Metal mould sample; (b) Firebrick mould sample

On the basis of classical solidification theory, grain size, on one hand, depends on the number of potentially efficient nuclei in the melt, and, on the other hand, is determined by the nucleation rate. Firstly, with the refinement of primary dendrite Al phases, it could influence both the distribution of nuclei for eutectic and the concentration in the liquid near the dendrite-liquid interface prior to the coupled growth of eutectic Al and eutectic Si phase. Secondly, some unknown potent nuclei for eutectic Si phase are easily activated in the undercooling melt, i.e., the number of eutectic nuclei is increased in unit time and unit volume of melt. Obviously, the time for meeting of grains or of lapping solute fields is shortened due to the increase of nucleus density, which restricts the growth of the eutectic cells in the time and space. Combining the results and analysis, it can be concluded that the evolution of primary dendrite Al phases affects remarkably the size, shape and distribution of eutectic cells.

Eventually, an important issue needs further to be clarified, is the modification mechanism of eutectic Si. Up to now, two predominant modification operating mechanisms have been put forward for explaining the modification behavior of eutectic Si [1]. The first, the effective nuclei for eutectic Si in melt are removed by modification elements based on the phenomenon of

increased nucleation undercooling, consequently, the solid-liquid eutectic interface advances at higher growth rate. The second, the interface structure of eutectic Si phase-liquid is changed by the modification elements based on the observation of high density growing twins, which would transform the growth manner of eutectic Si. The eutectic cells are refined significantly in a fully modified eutectic microstructure, as shown in Fig. 6. It can be speculated that the flake-fibrous transition of eutectic Si morphology involving in impurity modification may be independent of the frequency and mode of eutectic nucleation. The second modification mechanism seems to be supported by the present works.

4 Conclusions

1) The eutectic cell in hypoeutectic Al−Si is clearly revealed by an appropriate etching method. At the higher thermal gradient, the eutectic cells develop in a columnar manner, conversely, in an equiaxed manner. The growth of eutectic cells is in good agreement with the model of CET.

2) By EBSD mapping analysis, both the eutectic Si and Al phases in an eutectic cell are not single crystal, and an eutectic cell is composed of some small 'grains' with different crystallographic orientations. It is also suggested that the eutectic nucleation mode cannot be determined based on the crystallographic orientation between eutectic Al phases and the neighboring primary dendrite Al phases.

3) Refinement of primary dendrite Al phases could obviously improve the size, shape and distribution of eutectic cells. This indicates that the evolution of primary dendrite Al phases affects remarkably the following eutectic nucleation and growth.

4) The eutectic cells are refined significantly in a fully modified eutectic microstructure. It can be speculated that that the flake-fibrous transition of eutectic Si morphology involving in impurity modification may be independent of the frequency and mode of eutectic nucleation.

References

[1]   SUN Yu. Eutectic growth and precipitation strengthening of Al-Si alloy [D]. Nanjing: Southeast University, 2008. (in Chinese)

[2]   HOSCH T, NAPOLITANO R E. The effect of the flake to fiber transition in silicon morphology on the tensile properties of Al-Si eutectic alloys [J]. Materials Science and Engineering A, 2010, 528: 226−232.

[3]   JHA A K, SREEKUMAR K. Effect of pores and acicular eutectic silicon particles on the performance of Al-Si-Mg (AS7G03) casting [J]. Engineering Failure Analysis, 2009, 16: 2433−2439.

[4]   LU S Z, HELLAWELL A. The mechanism of silicon modification in aluminum-silicon alloys: Impurity induced twinning [J]. Metall Trans A, 1987, 18(10): 1721−1732.

[5]　BIAN X F, WANG W M, QIN J H. Structures of liquid Al-Si alloy modified by Sr [J]. Materials Science Forum, 2000, 331(1): 349−354.

[6]　MAKHLOUF M M, GUTHY H V. The aluminum-silicon reaction: mechanisms and crystallography [J]. Journal of Light Metals, 2001, 1: 199−218.

[7]　PRUKKANONA W, SRTSUKHUMBOWORNCHAIA N, LIMMANEEVICHITR C. Modification of hypoeutectic Al-Si alloys with scandium [J]. Journal of Alloys and Compounds, 2009, 477: 454−460.

[8]　NOGITA K, YOSHIDA K. Determination of strontium segregation in modified hypoeutectic Al-Si alloy by micro X-ray fluorescence analysis [J]. Scripta Materialia, 2006, 55: 787−790.

[9]　LIU C H, CHEN J H, LI C, WU C L, LI D C, LI D Z, LI Y Y. Multiple silicon nanotwins formed on the eutectic silicon particles in Al-Si alloys [J]. Scripta Materialia, 2011, 64: 339−342.

[10]　NOGITA K, DAHLE A K. Eutectic solidification in hypoeutectic Al-Si alloys: Electron backscatter diffraction analysis [J]. Mater Characterization, 2001, 46: 305−310.

[11]　DAHLE A K, NOGITA K, ZINDEL J K, McDONALD S D, HOGAN L M. Eutectic nucleation and growth in hypoeutectic Al-Si alloys at different strontium levels [J]. Metal and Mater Trans A, 2001, 32(4): 949−960.

[12]　SUMANTH S, YANCY W R, MAKHLOUF M. Nucleation mechanism of the eutectic phases in aluminum-silicon hypoeutectic alloys [J]. Acta Mater, 2004, 52: 4447−4460.

[13]　McDONALD S D, NOGITA K, DAHLE A K. Eutectic nucleation in Al-Si alloys [J]. Acta Mater, 2004, 52: 4273−4280.

[14]　McDONALD S D, DAHLE A K, TAYLOR J A, StJOHN D H. Eutectic grains in unmodified and strontium-modified hypoeutectic aluminum-silicon alloys [J]. Metal and Mater Trans, 2004, 35(6): 1829−1837.

[15]　LIAO Heng-cheng, WU Zhen-ping, DONG Guang-ming, CHEN Jie, SUN Guo-xiong. Effect of addition of Sr and B on the size eutectic cells in Al-15.5%Si alloy [J]. Acta Metallurgica Sinica, 2005, 41(10): 1047−1052. (in Chinese)

[16]　LIAO Heng-cheng, ZHANG, Min, WU Qi-chang, WANG Hui-pin, SUN Guo-xiong. Refinement of eutectic grains by combined addition of strontium and boron in near-eutectic Al-Si alloys [J]. Scripta Materialsia, 2007, 57: 1121−1124.

[17]　HUNT J D. Steady state columnar and equiaxed growth of dendrite and eutectic [J]. Mater Sci Eng, 1984, 65: 75−83.

[18]　LI Qing-chun. Fundamentals of casting forming [M]. Beijing: China Machine Press, 1982: 138−145. (in Chinese)

[19]　SUN Yu, WU Zheng-ping, LIU Bing-yi. Grain refinement for near-eutectic Al-Si alloys [J]. The Chinese Journal of Nonferrous Metals, 2004, 14(8): 1340−1347. (in Chinese)

亚共晶 Al−Si 合金共晶团的形核与生长

孙　瑜[1]，庞绍平[1]，刘学然[1]，杨子润[1]，孙国雄[2]

1. 盐城工学院 材料学院，盐城 224051；
2. 东南大学 材料学院，南京 210096

摘　要：采用光学显微镜、扫描电镜及电子背散射衍射技术研究亚共晶 Al−Si 合金共晶团的形核与生长。通过揭示共晶团和结晶位向的分析发现：在同一个共晶团中 Si 相和 Al 相都不是单晶体，而是由不同位向的小"晶粒"构成的。提出不能依据共晶团中 Al 相与周围初生枝晶 Al 相的位向关系来确定共晶的形核模式的建议。然而，初生枝晶铝相的演化显著影响随后的共晶形核与生长。涉及的杂质元素使共晶 Si 的形貌由粗大的片状转变成细小的纤维状的变质行为，可能与共晶的形核无关。

关键词：亚共晶 Al−Si 合金；共晶团；形核；生长

(Edited by YANG Hua)